Coordination-Dependent ESR Spectra of Copper(II) Complexes with a CuN_4 Type Coordination Mode: Relationship between ESR Parameters and Stability Constants or Redox Potentials of the Complexes[1)]

Takashi SAWADA, Katsuya FUKUMARU, and Hiromu SAKURAI*

Department of Analytical and Bioinorganic Chemistry, Kyoto Pharmaceutical University, Nakauchi-cho 5, Misasagi, Yamashina-ku, Kyoto 607, Japan. Received September 4, 1995; accepted January 10, 1996

ESR is useful for determining the unpaired electronic state around paramagnetic metal ions such as, copper(II), iron(III) and manganese(II). The coordination structure of Cu(II) complexes was examined by ESR. ESR spectra were measured for a series of polyamine Cu(II) complexes, whose coordination modes are square-planar, axially-coordinate square-planar, tetrahedral and distorted square-planar (copper ion displaced from N_4 plane). ESR parameters, *g*-values and hyperfine coupling constants, *A*-values, were found to be correlated with the coordination mode of the complex, in which *g vs. A* plots gave important information on coordination structure of the complex. Moreover, linear relationships between ESR parameters and stability constants or halfwave potentials of the Cu(II) complexes were observed. Based on these results, the coordination structure around the Cu(II) in copper complexes as well as copper proteins was predicted by ESR spectra and associated parameters.

Key words electron spin resonance; copper(II) complex; polyamine; coordination structure; stability constant; redox potential

Among essential trace elements, the transition metals such as copper, iron and manganese with several oxidation states play an especially important role in biochemical and physiological processes in living systems.[2,3)] Copper is widely distributed in nature, accounting for about 1.4—2.1 mg per kilogram of body weight in the adult human body.[3)] In general, copper ions in cells or blood are known to be present as low molecular weight copper complexes, copper proteins or copper enzymes. Among them, copper proteins play a central role as an oxygen carrier and a catalyst in oxidation–reduction reactions, oxygenation, and electron transfer.[4-6)] The functions of the copper proteins (enzymes) are clearly structure-related and thus it is very important to investigate the coordination structure of these proteins. To clarify the coordination structure of copper proteins, X-ray diffraction has been used. However, it is occasionally difficult to prepare a single crystal of copper protein (enzyme) suitable for X-ray diffraction. On the other hand, copper(II) has nine *d*-electrons in its outermost shell, in which the electronic configuration can be considered equivalent to one unpaired "hole." Thus, the electronic structure is simple and comparatively easy to study by ESR.[7)] Therefore, to determine the coordination structure of copper proteins in solution, X-band ESR has been used.[7,8)] For example, by plotting the ESR parameters $A_{\parallel}$-values and $g_{\parallel}$-values, information on the coordination structure of copper complexes can be obtained.[9,10)] Peisach and Blumberg reported that a decrease in the relative charge of the copper(II) complex produces a decrease in the $g_{\parallel}$-value but increases the hyperfine coupling constant $A_{\parallel}$-value.[9)] Further, Yokoi and Addison proposed that the $g_{\parallel}$-value increases but the $A_{\parallel}$-value decreases as the coordination structure of the copper(II) complex changes from square-planar to tetrahedrally distorted depending on the bulkiness of its substituent.[10)] These observations suggest that there is a close relationship between the coordination structure and the ESR parameters of copper(II) complexes.

To determine the coordination structure of a copper complex, both the stability and redox potential of the complex are important. However, the relationships between ESR parameters and stability constants or redox potentials have not been discussed in the literature. We have investigated the structure of copper(II) complexes by ESR spectroscopy, relating the ESR parameters to their overall stability constants ($\log K_{\beta}$, $K_{\beta}=[ML_n]/[M][L]_n$) and redox potentials. In this paper we report the results of an ESR study of CuN_4 type complexes, whose coordination modes are square-planar, axially-coordinate square-planar, tetrahedral or distorted square-planar (copper ion displaced from N_4-plane).

Experimental

Materials $Cu(II)SO_4 \cdot 5H_2O$, ammonia water and phen were purchased from Nacalai Tesque, Japan. En, dien, trien, tetren and hexen were obtained from Wako-Pure Chemical Industries, Japan. *N*-Me-en, *N,N*-Me_2-en, *N*-Et-en, tn, chxn and cyclen were from Tokyo Chemical Industry, Japan. *N,N'*-Me_2-en, *N*-Pr-en, bipy and cyclam were from Aldrich Chemicals, Germany. BSA was from Sigma Chemical, U.S.A. All ligands used are listed in Table 1.

Methods Solutions of the Cu(II) complexes were prepared by mixing ligands and $CuSO_4$ in aqueous solution. Concentrations were 5×10^{-4} at a molar ratio of Cu : ligand = 1 : 0.5—1 : 8. The pH was adjusted to 7.4 with phosphate buffer (0.1 M K_2HPO_4–0.1 M KH_2PO_4) or 2,6-lutidine–HCl buffer (0.01 M 2,6-lutidine–0.1 M HCl).

ESR spectra were recorded with an X-band ESR spectrometer, JES-RE3X, JEOL, Japan, at room temperature (22 °C) or at liquid nitrogen temperature (77 K). Instrumental conditions for the ESR measurements were as follows: Modulation frequency 100 kHz, modulation amplitude 0.63 mT and microwave power 5 mW. The *g*-values of the complexes were calibrated using two standards, Li-TCNQ ($g=2.00252$) and Mn(II) in MgO ($\Delta H_{3-4}=8.69$ mT). The α^2-value for Cu(II) complexes was calculated from ESR parameters using the equation of Kivelson and Neiman ($\alpha^2 = A_{\parallel}/P + (g_{\parallel} - 2.0023) + 3/7(g_{\perp} - 2.0023) + 0.04$, $P = 360\,cm^{-1}$).[11)]

Visible absorption spectra of aqueous solutions were recorded at room temperature on a UV-260 spectrophotometer, Shimazu, Japan. Concentrations were 1×10^{-2} M at a molar ratio of Cu : ligand = 1 : 4 and the pH (4—11) was adjusted using 0.1 M NaOH and 0.1 M HCl.

Cyclic voltammograms were obtained for a solution of acetonitrile–water (1 : 1) containing 0.1 M tetra-*n*-butyl-ammonium perchlorate using

* To whom correspondence should be addressed.

an electrochemical workstation, 100B/W, BAS, U.S.A. Concentrations were 1×10^{-3} M at a molar ratio of Cu : ligand = 1 : 2. Cyclic voltammetry was performed with a three-electrode system containing a glassy-carbon working electrode, a platinum counter electrode and an Ag/AgCl (saturated NaCl) reference electrode. Cyclic voltammograms were recorded at a scan rate of 100 mV s^{-1}. Halfwave potential $E_{1/2}$ values were determined as the midpoint between the peak potentials, $E_{1/2} = (E_{pc} + E_{pa})/2$. Redox potentials were calculated using the following equation, $E°(\text{NHE}) = E_{1/2}(\text{Ag/AgCl}) + 212$ (mV).

Magnetic susceptibility and mass susceptibility for powder (χ_g) or aqueous solution (χ_s) were measured at room temperature (25 °C) with a magnetic susceptibility balance, MK-I, Sherwood Scientific, U.K. The concentration was 0.1 M at a molar ratio of Cu : ligand = 1 : 4. The χ_g-value of the solute was obtained from the following relationship: $\chi_s = (m_1/(m_1+m_2)) \times \chi_g + (m_2/(m_1+m_2)) \times \chi_0$, where m_1 and m_2 are weights (grams) of solute and solvent, respectively, and χ_0 is the mass susceptibility of the solvent. The χ_0-value was obtained separately. Numbers of unpaired electrons were calculated using the equation, $\mu_{eff} = [n(n+2)]^{1/2}$, where μ_{eff} is the magnetic moment and n is the number of unpaired electrons. Mass susceptibility χ_g, molar susceptibility χ_m and susceptibility per gram atom of the paramagnetic ion χ_a were measured.

Results

ESR Spectra ESR spectra were obtained at both room (22 °C) and liquid nitrogen (77 K) temperatures. Sample solutions of Cu(II) complexes with bidentate or tridentate ligands at a molar ratio of Cu : ligand = 1 : 1 showed complicated ESR spectra, indicating the formation of complexes composed of 1 : 1 and 1 : 2 ratios of Cu(II) to ligand.[1,2] When the molar ratio of ligand to Cu(II) ion increased, ESR spectra showing the formation of a complex due to a single species were obtained. However, Cu(II) complexes with 4-, 5- and 6-dentate ligands gave ESR spectra due to a single species at a molar ratio of Cu : ligand = 1 : 1. Three typical types of ESR spectra for Cu(II) complexes at pH 7.4 are shown in Fig. 1. The parallel components, $g_{\parallel}$ and $A_{\parallel}$, were determined from the spectra at low-temperature. However, the perpendicular components, $g_{\perp}$ and $A_{\perp}$, were not determined exactly. Since the average values, g_0 and A_0, are determined from the ESR spectra for a Cu(II) complex in free tumbling motion at room temperature, $g_{\perp}$ and $A_{\perp}$ can be calculated from the following relationships, $g_0 = (g_{\parallel} + 2g_{\perp})/3$ and $A_0 = (A_{\parallel} + 2A_{\perp})/3$. The ESR parameters of the Cu(II) complexes thus obtained are summarized in Table 1, where the indicated configurations of the complexes are estimated from the reported results of X-ray

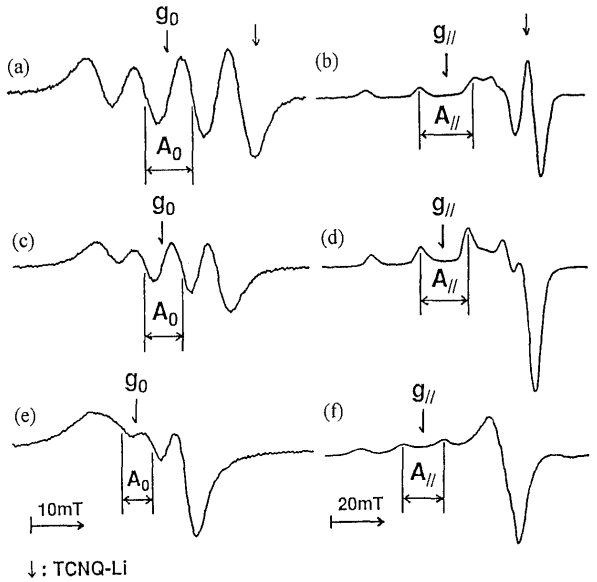

Fig. 1. Typical X-Band ESR Spectra for Cu(II) Complexes at pH 7.4

(a) Cu(II)–$(en)_2$ at room temperature, (b) Cu(II)–$(en)_2$ at liquid nitrogen temperature (77 K), (c) Cu(II)–$(dien)_2$ at room temperature, (d) Cu(II)–$(dien)_2$ at liquid nitrogen temperature, (e) Cu(II)–$(phen)_2$ at room temperature, (f) Cu(II)–$(phen)_2$ at liquid nitrogen temperature.

Table 1. ESR Parameters for Polyamine–Cu(II) Complexes at pH 7.4 with CuN_4 Type Coordination Mode

Ligand	g-value			A-value (10^4 cm^{-1})			log K_β[a]	λ_{max}	ε	α^2
	g_0	$g_{\parallel}$	$g_{\perp}$	A_0	$A_{\parallel}$	$A_{\perp}$		(nm)	(M^{-1} cm^{-1})	
Square-planar										
$(en)_2$[d]	2.101	2.204	2.050	82.9	209.5	23.8	19.6	547	128	0.84
(*N*-Me-en)$_2$[e]	2.104	2.208	2.052	83.2	203.2	27.3	18.9	551	84	0.83
(*N*,*N*-Me_2-en)$_2$	2.104	2.203	2.055	80.3	200.0	24.4	16.4	564	156	0.82
(*N*,*N'*-Me_2-en)$_2$	2.106	2.214	2.052	82.8	200.3	28.2	17.1	565	107	0.83
(*N*-Et-en)$_2$[f]	2.104	2.208	2.052	82.4	202.1	26.7	18.6	558	112	0.83
(*N*-Pr-en)$_2$	2.104	2.207	2.053	82.2	200.3	27.1	18.1	559	104	0.82
$(tn)_2$[g]	2.109	2.220	2.054	78.6	202.6	21.1	16.9	568	106	0.84
$(chxn)_2$	2.103	2.205	2.052	84.0	206.7	26.7	20.4	542	76	0.84
cyclam[h]	2.093	2.185	2.047	89.9	216.1	30.7	27.2	583	108	0.84
$(NH_3)_4$[b,j]	2.122	2.248	2.059	76.2	188.6	24.5	13.0	596	52	0.83
$(py)_4$[c,j]	2.133	2.304	2.048	72.1	185.8	21.2	6.5	559	104	0.88
Axially-coordinate square-planar										
$(dien)_2$[k] (6-coordinate)	2.113	2.212	2.064	65.4	181.7	11.1	20.9	630	110	0.78
hexen[p] (5-coordinate)	2.110	2.203	2.064	66.7	167.6	19.3	22.1	627	236	0.73
tetren[p] (5-coordinate)	2.110	2.205	2.063	66.7	163.2	21.4	22.8	645	166	0.72
Tetrahedral										
$(phen)_2$[l]	2.145	2.271	2.082	57.3	155.8	12.0	11.1	690	42	0.78
$(bipy)_2$[m]	2.145	2.259	2.088	59.5	156.1	14.7	12.7	700	72	0.77
Distorted square-planar										
trien[n]	2.102	2.200	2.053	80.8	200.2	24.9	20.1	587	144	0.82
cyclen[o]	2.103	2.200	2.054	76.0	191.3	22.1	24.8	605	202	0.79

a) A. E. Martell, Critical Stability Constants, vol. 2 Amines, vol. 5 First Supplement (1982). *b*) In the presence of excess aqueous ammonia. *c*) In the presence of excess pyridine (Cu : py = 1 : 100). *d*) See ref. 13—15, *e*) see ref. 16, *f*) see ref. 17, *g*) see ref. 18—20, *h*) see ref. 15, 21, *i*) see ref. 22, *j*) see ref. 23, *k*) see ref. 24—26, *l*) see ref. 27, *m*) see ref. 28, *n*) see ref. 29, *o*) see ref. 30, *p*) see ref. 34.

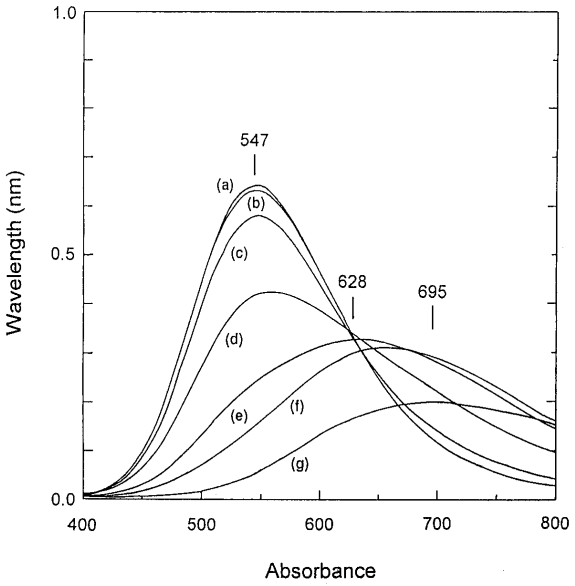

Fig. 2. pH-Dependent Visible Absorption Spectral Change for the Cu(II)–$(en)_2$ Complex

The complex was prepared at a molar ratio of Cu(II) : ligand = 1 : 4 (Cu(II) = 10 mM). (a) pH 7—11, (b) pH 6, (c) pH5.5, (d) pH 5, (e) pH 4.7, (f) pH 4.5, (g) pH 4.

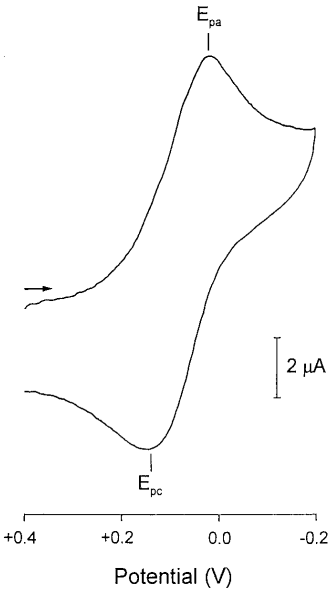

Fig. 3. Cyclic Voltammogram for the Cu(II)–$(bipy)_2$ Complex in Acetonitrile–Water (1 : 1) Containing 0.1 M Tetra-*n*-butyl Ammonium Perchlorate

The complex was prepared at a molar ratio of Cu(II) : ligand = 1 : 2 (Cu(II) = 1 mM).

crystal analyses.[13-30]

Visible Absorption Spectra When the structures of the Cu(II) complexes change from square-planar to axially-coordinate square-planar, tetrahedral and distorted square-planar (Cu ion displaced from N_4 plane), red shifts due to *d–d* transitions are observed,[10,31,32] as indicated by the results with Cu(II)–*N*-alkylsalicylaldiminate complexes.[33] Typical pH-dependent visible absorption spectra for the Cu(II)–$(en)_2$ complex are shown in Fig. 2 and the visible absorption parameters at pH 7—11 are summarized in Table 1. Most complexes tested gave an absorption peak at 550—700 nm ($\varepsilon < 300\ M^{-1}\,cm^{-1}$).

Halfwave Potentials Figure 3 shows a typical cyclic voltammogram for the Cu(II)/Cu(I) coupled reaction in the Cu(II)–$(bipy)_2$ complex. The cyclic voltammogram displayed a typical quasi-reversible redox-reaction at $E_{1/2}$ (*vs.* Ag/AgCl electrode). Table 2 summarizes the electrochemical data for the Cu(II) complexes tested.

Table 2. Electrochemical Data for Cu(II) Complexes in Acetonitrile–Water (1 : 1)

Ligand	Electrochemical parameters			ESR parameters	
	E_{pc} (mV)	E_{pa} (mV)	$E_{1/2}$ (mV)	$g_{\parallel}$	$A_{\parallel}$ ($10^{-4}\,cm^{-1}$)
Square-planar					
$(en)_2$	−472	−353	−413	2.204	209.5
$(N\text{-Me-en})_2$	−445	−310	−378	2.208	203.2
$(N,N\text{-Me}_2\text{-en})_2$	−257	−145	−201	2.203	200.0
$(N,N'\text{-Me}_2\text{-en})_2$	−332	−188	−260	2.214	200.3
$(N\text{-Et-en})_2$	−332	−222	−277	2.208	202.1
$(N\text{-Pr-en})_2$	−302	−196	−249	2.207	200.3
$(tn)_2$	−338	−241	−290	2.220	202.6
$(chxn)_2$	−541	−455	−498	2.205	206.7
cyclam	−992	−915	−954	2.185	216.1
$(NH_3)_4$[a]	−126	−18	−72	2.248	188.6
$(py)_4$[b]	+229	+338	+284	2.304	185.8
Axially-coordinate square-planar					
$(dien)_2$ (6-coordinate)	−509	−409	−459	2.212	181.7
hexen (5-coordinate)	−662	−571	−617	2.203	167.6
tetren (5-coordinate)	−697	−617	−657	2.205	163.2
Tetrahedral					
$(bipy)_2$	+33	+127	+80	2.259	156.1
$(phen)_2$	+6	+103	+55	2.271	155.8
Distorted square-planar					
trien	−561	−473	−517	2.200	200.2
cyclen	−646	−588	−617	2.200	191.3

a) In the presence of excess aqueous ammonia, scan rate of $400\,mV\,s^{-1}$. *b*) In the presence of excess pyridine (Cu : py = 1 : 100).

Magnetic Susceptibilities The magnetic susceptibility of a Cu(II) complex in solution is very useful for determining the electronic state of the complex. We measured the magnetic susceptibility of Cu(II)–$(AcO)_2$ in both solid state and 0.1 M AcOH solution (pH 4.4). At Cu(II) concentration of 0.1 M or above, an $\chi_g = 5.17 \times 10^{-6} \pm 2.41 \times 10^{-7}$ c.g.s. was found, similar to that ($4.23 \times 10^{-6} \pm 5.09 \times 10^{-8}$ c.g.s.) in the solid state complex. Then, the magnetic susceptibility of an aqueous solution at pH 10 together with that of a powder of the CuN_4 type complexes was measured and the results are summarized in Table 3. All complexes showed magnetic moments of 1.65—1.85 B. M., indicating that all complexes have one unpaired electron in the paramagnetic state, the theoretical value being 1.73 B. M.

Discussion

Relationship between ESR Parameters and Stability Constants or Halfwave Potentials for Cu(II) Complexes Coordination structures of CuN_4 type complexes were examined in terms of their ESR parameters. The configuration of the Cu(II) complexes was assigned by X-ray crystallographic analyses.[13-30] Both configurations of Cu(II)–tetren and Cu(II)–hexen in solution have been indicated to be in the five coordination mode, since their stability constants are higher than that of the Cu(II)–trien complex.[34] Thus, we assigned the configurations of

Table 3. Magnetic Susceptibility for CuN_4 Type Complexes in Aqueous Solution at pH 10

Ligand	Magnetic parameters			
	χ_g ($\times 10^{-6}$ c.g.s.)	χ_m ($\times 10^{-3}$ c.g.s.)	χ_a ($\times 10^{-3}$ c.g.s)	μ_{eff}
Square-planar				
$(en)_2$[a]	3.954	1.249	1.407	1.82
$(N\text{-Me-en})_2$	3.539	1.089	1.238	1.72
$(N,N\text{-Me}_2\text{-en})_2$	3.038	1.021	1.195	1.69
$(N,N'\text{-Me}_2\text{-en})_2$	2.992	1.005	1.178	1.68
$(N\text{-Et-en})_2$	3.153	1.059	1.234	1.71
$(N\text{-Pr-en})_2$	3.071	1.118	1.312	1.77
$(tn)_2$	3.427	1.055	1.208	1.70
$(NH_3)_4$[b]	4.744	1.080	1.170	1.67
$(py)_4$[c]	2.331	1.110	1.344	1.79
Axially-coordinate square-planar				
$(dien)_2$ (6-coordinate)	2.971	1.087	1.278	1.75
hexen (5-coordinate)	2.410	0.945	1.145	1.65
tetren (5-coordinate)	3.050	1.064	1.236	1.72
Tetrahedral				
$(bipy)_2$[a]	1.967	1.131	1.381	1.81
$(phen)_2$[a]	2.263	1.177	1.441	1.85
Distorted square-planar				
trien	3.380	1.034	1.176	1.67
cyclen	3.480	1.155	1.311	1.77

a) Data of crystalline, *b*) in the presence of excess aqueous ammonia, *c*) in the presence of excess pyridine (Cu : py = 1 : 50).

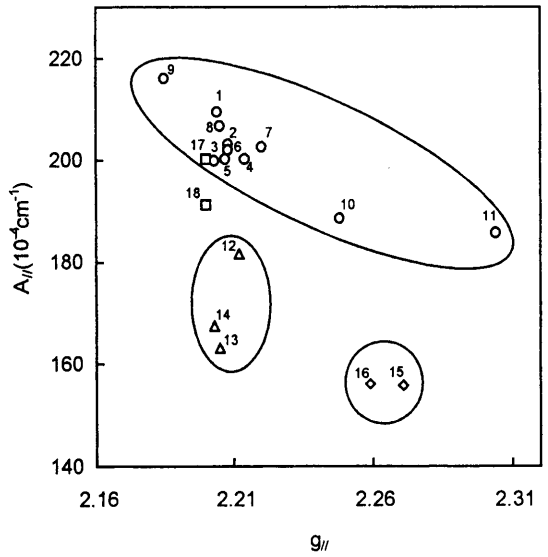

Fig. 4. Relationship between $g_{\parallel}$-Values and $A_{\parallel}$-Values for a CuN_4 Type Complex

(○) square-planar, (△) axially-coordinate square-planar, (◇) tetrahedral, (□) distorted square-planar. 1. $(en)_2$; 2. $(N\text{-Me-en})_2$; 3. $(N,N\text{-Me}_2\text{-en})_2$; 4. $(N,N'\text{-Me}_2\text{-en})_2$; 5. $(N\text{-Et-en})_2$; 6. $(N\text{-Pr-en})_2$; 7. $(tn)_2$; 8. $(chxn)_2$; 9. cyclam; 10. $(NH_3)_4$; 11. $(py)_4$; 12. $(dien)_2$; 13. tetren; 14. hexen; 15. $(phen)_2$; 16. $(bipy)_2$; 17. trien; 18. cyclen.

the Cu(II)–hexen and –tetren complexes as axially-coordinate square-planar. Other physicochemical properties of the Cu(II) complexes were characterized by their visible absorption spectra, halfwave potentials and magnetic susceptibilities. The relationship of the ESR parameters, $A_{\parallel}$-values *vs.* $g_{\parallel}$-values, for Cu(II) complexes is shown in Fig. 4. Square-planar complexes have relatively large $A_{\parallel}$-values compared with those for complexes in other coordination modes. On the other hand, plots of axially-

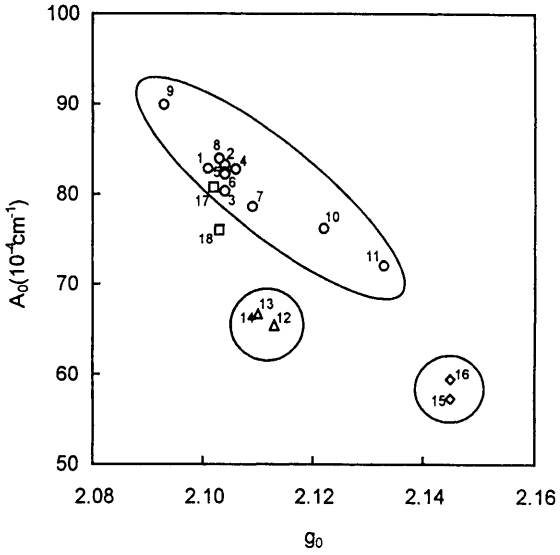

Fig. 5. Relationship between g_0-Value and A_0-Value for a CuN_4 Type Complex

(○) square-planar, (△) axially-coordinate square-planar, (◇) tetrahedral, (□) distorted square-planar. 1—18: See the caption of Fig. 4.

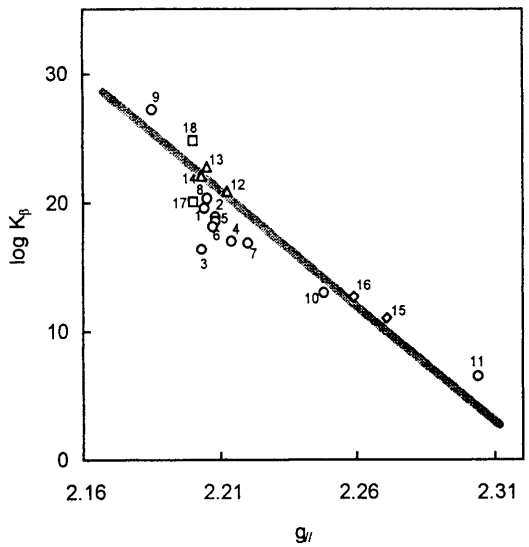

Fig. 6. Relationship between $g_{\parallel}$-Value and $\log K_\beta$ for a CuN_4 Type Complex

(○) square-planar, (△) axially-coordinate square-planar, (◇) tetrahedral, (□) distorted square-planar. Correlation coefficient of linear regression was $r = 0.911$ for a total of 18 points. 1—18: See the caption of Fig. 4.

coordinate square-planar and tetrahedral complexes having small $A_{\parallel}$-values show a different distribution from those for square-planar complexes. Similarly, plots A_0-*vs.* g_0-value was also found to depend on the coordination structure of the Cu(II) complexes (Fig. 5).

Square-planar complexes appear to show a linear relationship in plots of *A*- *vs.* *g*-value (Fig. 4), suggesting that this relationship may correlate with the stability of the complexes. When $g_{\parallel}$-values were plotted against the overall stability constants ($\log K_\beta$, $K_\beta = [ML_n]/[M][L]_n$) of the complexes with various coordination modes, a good linear relationship with the correlation coefficient $r = 0.911$ for the linear regression for a total of 18 points, was found as shown in Fig. 6; however, the $A_{\parallel}$-value correlated linearly (correlation coefficient $r = 0.951$ for a total of 11

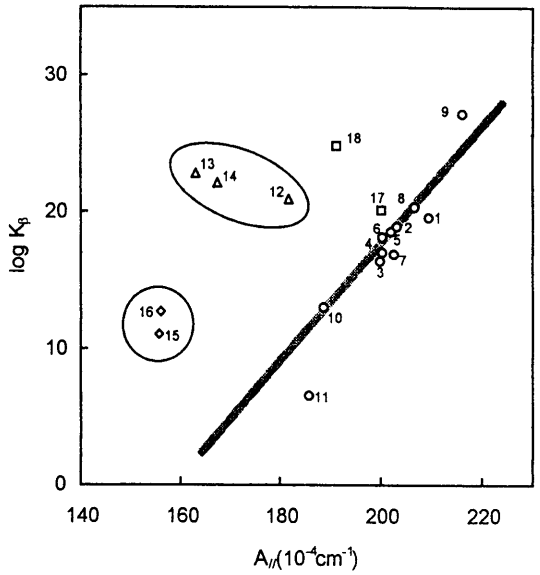

Fig. 7. Relationship between $\log K_\beta$ and $A_{\parallel}$-Value for a CuN_4 Type Complex

(○) square-planar, (△) axially-coordinate square-planar, (◇) tetrahedral, (□) distorted square-planar. Correlation coefficient of linear regression for the square-planar type complexes was $r=0.951$ for a total of 11 points. 1—18: See the caption of Fig. 4.

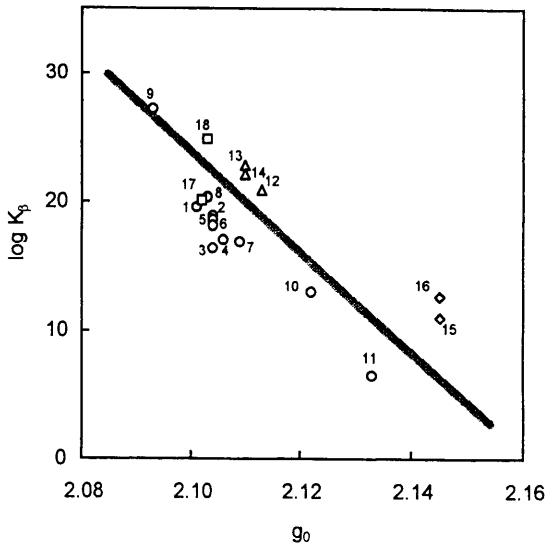

Fig. 8. Relationship between g_0-Value and $\log K_\beta$ for a CuN_4 Type Complex

(○) square-planar, (△) axially-coordinate square-planar, (◇) tetrahedral, (□) distorted square-planar. Correlation coefficient of linear regression was $r=0.783$ for a total of 18 points. 1—18: See the caption of Fig. 4.

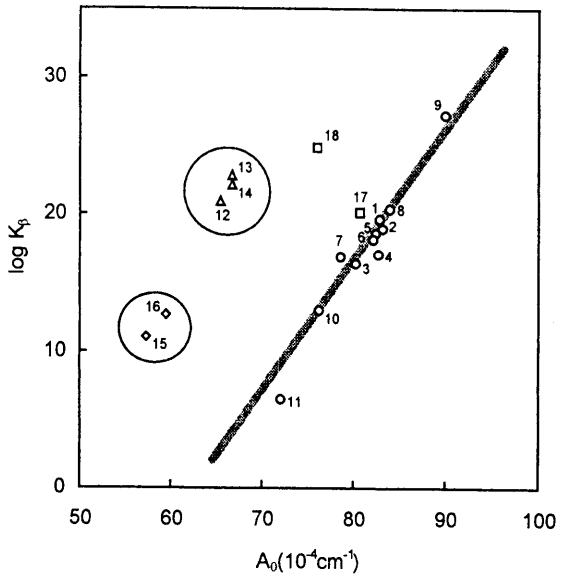

Fig. 9. Relationship between $\log K_\beta$ and A_0-Value for a CuN_4 Type Complex

(○) square-planar, (△) axially-coordinate square-planar, (◇) tetrahedral, (□) distorted square-planar. Correlation coefficient of linear regression for the square-planar type complexes was $r=0.975$ for a total of 11 points. 1—18: See the caption of Fig. 4.

points) with $\log K_\beta$ only for the square-planar complexes (Fig. 7). The pK_a-values of ligands in Cu(II) complexes have been reported to be linearly related to the $g_{\parallel}$-value, *e.g.* the β-diketone chelates of Cu(II).[35] However, as far as we know, the stability constant of metal complexes has not been shown to be related to the ESR parameters (g- and A-value). The stability constant of a complex is considered to relate to the electron donating ability from ligand to metal.[35] The complex which has a high stability constant possesses a high electron density at the Cu(II) site. Therefore, as the stability constant increases, the A-value increases and the g-value decreases. In the present study, the A-value was also shown to be influenced by a change in the coordination structure. In fact, the square-planar type complexes showed a good linear relationship between the $A_{\parallel}$-value and $\log K_\beta$, but the other complexes did not (Fig. 7). On the other hand, the $g_{\parallel}$-value was not influenced by a change in the coordination structure. Thus, it is thought that the $g_{\parallel}$-value is mainly affected by the electron density on the Cu(II). In addition, at room temperature, similar good relationships to those at liquid nitrogen temperature were observed, when the g_0- or A_0-values are plotted against the $\log K_\beta$ values (correlation coefficients $r=0.783$ and 0.975 for a total of 18 and 11 points, respectively) (Figs. 8, 9). In general, the structures of Cu(II) complexes in the solution state at room temperature and in the frozen state at 77 K are supposed to be different, and this problem has not been discussed to date. However, the finding of good relationships between the $\log K_\beta$ and g-values or A-values at both temperatures makes it reasonable to presume that the Cu(II) complexes formed have the same structures in spite of the difference in temperature. These results should be very useful for investigating the structures of the Cu(II) complexes at room temperature by other methods such as low-frequency L-band ESR spectroscopy.

To analyze the ESR parameters in more detail, we calculated the α^2-value (Table 1), which evaluates unpaired-electron density on the d-orbital of the Cu(II) ion as proposed by Kivelson and Neiman.[11] Square-planar complexes with large A-values had relatively large α^2-values, while axially-coordinated square-planar and tetrahedral complexes with small A-values had small α^2-values, indicating that α^2-values relate closely to A-values.

The E°-value of the Cu(II)/Cu(I) couple may relate to the destabilization of the Cu(II) species by (a) steric hindrance of ligands or (b) reduction of CFSE by constraining the geometry of the metal center to those

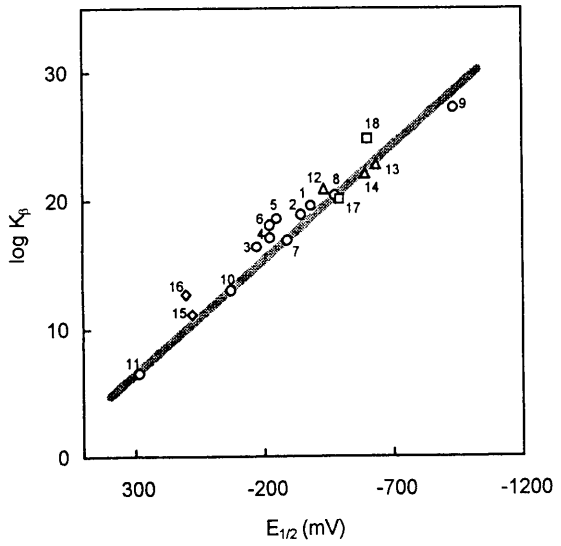

Fig. 10. Relationships between $E_{1/2}$ and $\log K_\beta$ for CuN_4 Type Complexes

(○) square-planar, (△) axially-coordinate square-planar, (◇) tetrahedral, (□) distorted square-planar. Correlation coefficient of linear regression was $r=0.976$ for a total of 18 points. 1—18: See the caption of Fig. 4.

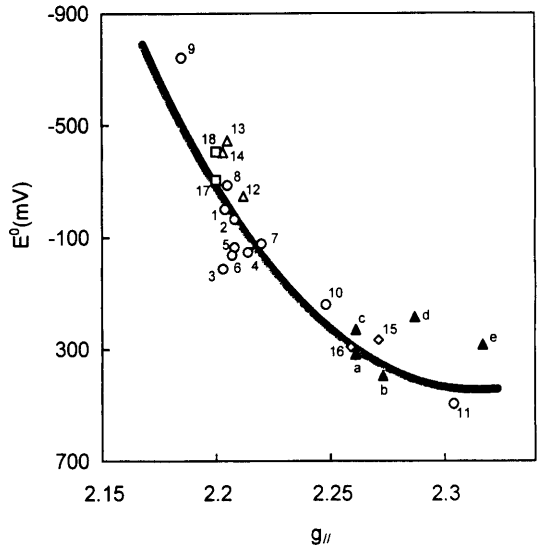

Fig. 11. Relationships between $g_{||}$-Value and $E_{1/2}$ for CuN_4 Type Complexes Involving Several Copper Proteins[43-53]

(○) square-planar, (△) axially-coordinate square-planar, (◇) tetrahedral, (□) distorted square-planar. Correlation coefficient of quadric curve regression was $r=0.906$ for a total of 18 points (low-molecular weight Cu(II) complexes). 1—18: See the caption of Fig. 4. a. azurin (*pseudomonas aeruginosa*)[44,45]; b. azurin (*bordatella bronchiseptica*)[46,47]; c. azurin (*pseudomonas denitrificans*)[44,48,49]; d. stellacyanin (pH 7.0)[50,51]; e. umecyanin[52,53]

with low CFSE, which conversely usually favors the Cu(I) state.[10,36] Cu(II) complexes of *N*-alkyl-ethylenediamines had relatively more positive halfwave potentials than that of the Cu(II)–$(en)_2$ complex because of the destabilization through the steric hindrance of the other alkyl substituents. Complexes of 5- or 6-dentate ligands, such as hexen or tetren respectively, had relatively negative halfwave potentials due to their high stability derived from chelate or entropy effects.[34,37,38] In contrast, tetrahedral complexes such as Cu(II)–$(phen)_2$ or –$(bipy)_2$ had positive halfwave potentials compared with those of square-planar complexes, probably due to the low CFSE of the ligand. Since halfwave potentials are closely related to the electron density on the Cu(II) atom, a Cu(II) complex which has a more negative halfwave potential is difficult to reduce to Cu(I) compared with the complex which has a more positive halfwave potential. Therefore, Cu(II) complexes which have relatively negative halfwave potentials possess a high electron density on Cu(II) atom. Plotting the halfwave potential *vs.* the stability constant for the complexes gave a good linear relationship with a correlation coefficient $r=0.976$ for a total of 18 points (Fig. 10), indicating that stability constants are related to the electron density at the metal center. These results support a relationship between ESR parameters and stability constants. Moreover, the $g_{||}$-value and halfwave potential have been reported to be correlated,[10,39,40] however in the present study we found a quadric curve regression ($r=0.906$ for a total of 18 points) as shown in Fig. 11. From these results, it is concluded that the ESR parameters, overall stability constants and halfwave potentials of the Cu(II) complexes are related to each other in terms of the electron density on Cu(II) center.

Coordination-Dependent ESR Spectral Pattern Recognition In the present investigation, we examined the ESR for complexes having various coordination configurations such as square-planar,[13-23] axially-coordinate square-planar,[24-26] tetrahedral[27,28] and distorted square-planar[29,30] based on the reported analyses of X-ray crystallographic data. From the spectral patterns of these complexes, shown in Fig. 1, the following results were deduced. The spectra for the square planar complexes at liquid nitrogen temperature have two deep troughs at high magnetic field (Fig. 1b). The ESR spectrum of the stellacyanin–Cu(II) complex which has a square-planar configuration at pH 12.8[41] belongs to the group of square-planar complexes. The spectra for axially-coordinate square-planar complexes at liquid nitrogen temperature show a small trough at low magnetic field and a second deep trough at high magnetic field (Fig. 1d). The bleomycin–Cu(II) complex gives an ESR spectral pattern associated with axially-coordinated complexes.[39] In contrast, the spectra for the tetrahedrally distorted complexes give only a deep trough at 77 K (Fig. 1f). At both room and liquid nitrogen temperatures, spectra for the tetrahedrally distorted complexes shifted to a low-magnetic field compared with those for square-planar complexes. This spectral pattern is found in the ESR spectrum of superoxide dismutase which has a tetrahedrally distorted configuration.[42] The distorted square-planar complexes in which the copper ion is displaced from the N_4 plane formed by ligands show a similar spectral pattern to those of the square-planar complexes. From these observations, it is possible to determine the coordination structure around the Cu(II) from the ESR spectral pattern of the complex.

Conclusion

Copper is an important essential trace metal in living systems where the water is about 70—80% of body weight. Most copper ions exist as copper proteins or enzymes and to understand the functions of these copper proteins, it is essential to know the coordination structure of the copper

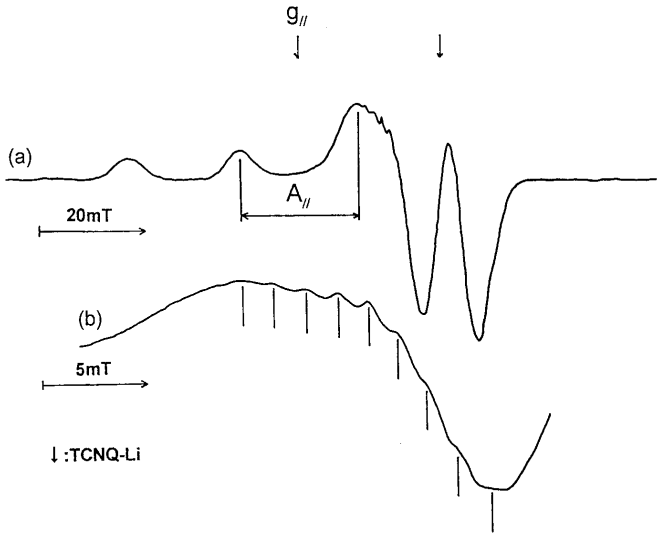

Fig. 12. X-Band ESR Spectra for the Cu(II)–BSA Complex

(a) Spectrum at pH 9.2 in 0.1 M KH_2PO_4–0.05 M $Na_2B_4O_7$ buffer at liquid nitrogen temperature (77 K). (b) Expanded region at the high magnetic field in spectrum (a). The 9-line superhyperfine structure seen in the spectrum is due to the formation of the CuN_4 center.

binding sites in aqueous systems.

In this investigation, we found that X-band ESR is valuable for estimating the configuration of Cu(II) complexes in terms of ESR parameters as well as ESR spectral patterns. For example, the Cu(II)–BSA complex (Cu : BSA = 1 : 1) at pH 9.2 in 0.1 M KH_2PO_4–0.05 M $Na_2B_4O_7$ buffer had a square-planar type ESR spectral pattern (Fig. 12a) giving ESR parameters: $g_{\parallel} = 2.176$ and $A_{\parallel}\,(cm^{-1}) = 221.79 \times 10^{-4}$. Detection of ligand superhyperfine splitting ($A_N = 1.45$ mT), consisting of a 9-line signal (Fig. 12b), demonstrates that four nitrogen ligand atoms (^{14}N, $I = 1$) coordinate with the Cu(II) ion. Therefore, the Cu(II)–BSA complex could be presumed to have a square-planar configuration at pH 9.2. Moreover, when the data on the Cu(II) proteins[43] were added to those in Fig. 11, a quadric relationship between the $g_{\parallel}$-value and halfwave potential was also observed, supporting the correlation found for the Cu(II) complexes with low molecular weight. The relationship between the $g_{\parallel}$-value and halfwave potential may be useful for estimating a parameter like the $g_{\parallel}$-value or halfwave potential when one is known. Thus, X-band ESR has been shown to be useful for determining the Cu(II) coordination site together with several physicochemical parameters of a Cu(II) complex, protein or enzyme, whose structure is unknown.

Acknowledgment This work was partially supported by grants from the Ministry of Education, Science and Culture of Japan.

References and Notes

1) Abbreviations: AcOH (acetic acid), en (ethylenediamine), *N*-Me-en (*N*-methylethylenediamine), *N*,*N*-Me_2-en (*N*,*N*-dimethylethylenediamine), *N*,*N*′-Me_2-en (*N*,*N*′-dimethylethylenediamine), *N*-Et-en (*N*-ethylethylenediamine), *N*-Pr-en (*N*-propylethylenediamine), tn (1,3-trimethylenediamine), chxn (*trans*-1,2-cyclohexanediamine), dien (diethylenetriamine), trien (triethylenetetramine), tetren (tetraethylenepentamine), hexen (pentaethylenehexamine), phen (1,10-phenanthroline), bipy (2,2′-bipyridine), cyclen (1,4,7,10-tetraazacyclododecane tetrahydrochloride), cyclam (1,4,8,11-tetraazacyclotetradecane), Li-TCNQ (tetracyano quinodimethane lithium salt), BSA (bovine serum albumine), ESR (electron spin resonance), E_{pa} (oxidation potential), E_{pc} (reduction potential), $E°$ (redox potential), $E_{1/2}$ (halfwave potential), NHE (normal hydrogen electrode), χ_g (mass susceptibility), χ_s (mass susceptibility of solution), χ_0 (mass susceptibility of solvent), χ_m (molar susceptibility), χ_a (susceptibility per gram atom of the paramagnetic ion), μ_{eff} (magnetic moment), $\log K_{\beta}$ (over-all stability constant), CFSE (crystal field stabilization energy), I (magnetic quantum number).
2) Underwood E. J., "Trace Elements in Human and Animal Nutrition," 3rd Ed., Academic Press, New York, 1978, pp. 57—115.
3) Sorenson J. R. J., *Prog. Med. Chem.*, **26**, 437—568 (1989).
4) Boas J. F., Pilbrow J. R., Smith T. D., *Biological Magnetic Resonance*, **1**, 277—342 (1978).
5) Kitajima N., *Adv. Inorg. Chem.*, **39**, 1—77 (1992).
6) Karlin K. D., *Science*, **261**, 701—708 (1993); Solomon E. I., Lowery M. D., *ibid.*, **259**, 1575—1581 (1993).
7) Vänngård T., "Biological Applications of Electron Spin Resonance," ed. by Swartz H. M.; Bolton J. R., Borg D. C., Wiley-Interscience, New York, **1972**, pp. 411—447.
8) Malmström B. G., Mosbach R., Vänngård T., *Nature* (London), **183**, 321—322 (1959).
9) Peisach J., Blumberg W. E., *Arch. Biochem. Biophys.*, **165**, 691—708 (1974).
10) Yokoi H., Addison A. W., *Inorg. Chem.*, **16**, 1341—1349 (1977).
11) Kivelson D., Neiman R., *Chem. Phys.*, **35**, 149—155 (1961).
12) Yokoi H., Otagiri M., Isobe T., *Bull. Chem. Soc. Jpn.*, **46**, 442—447 (1973).
13) Komiyama Y., Lingafelter E. C., *Acta Crystallogr.*, **17**, 1145—1148 (1964).
14) Brown B. W., Lingafelter E. C., *Acta Crystallogr.*, **17**, 254—259 (1964).
15) Emsley J., Arif M., *J. Mol. Struct.*, **220**, 1—12 (1990).
16) Luukkonen E., Pajunen A., *Suom. Kemistil. B*, **42**, 474—477 (1969).
17) Grenthe I., Paoletti P., Sandström M., Glikberg S., *Inorg. Chem.*, **18**, 2687—2692 (1979).
18) Pajunen A., *Suom. Kemistil. B*, **42**, 15—18 (1969).
19) Pajunen A., Belinskij I., *Suom. Kemistil. B*, **43**, 70—74 (1970).
20) Uggla A., Klinga M., *Suom. Kemistil. B*, **45**, 10—15 (1972).
21) Addison A. W., Sinn E., *Inorg. Chem.*, **22**, 1225—1228 (1983).
22) Mazzi F., *Acta Crystallogr.*, **8**, 137—141 (1955).
23) Maekawa M., Munakata M., Kitagawa S., Nakamura M., *Anal. Sci.*, **7**, 827—828 (1991).
24) Hathaway B. J., Bew M. J., Billing D. E., Dudley R. J., Nicholls P., *J. Chem. Soc., A*, **1969**, 2312—2318.
25) Stephens F. S., *J. Chem. Soc., A*, **1969**, 2233—2241.
26) Stephens F. S., *J. Chem. Soc., A*, **1969**, 883—890.
27) Nakai H., *Bull. Chem. Soc. Jpn.*, **56**, 1637—1641 (1983).
28) Amournjarusiri K., Hathaway B. J., *Acta Crystallogr., Sect. C*, **47**, 1383—1385 (1991).
29) Marongiu G., Lingafelter E. C., Paoletti P., *Inorg. Chem.*, **8**, 2763—2767 (1969).
30) Clay R., Murray-Rust P., Murray-Rust J., *Acta Crystallogr., Sect. B*, **35**, 1894—1895 (1979).
31) Murakami Y., Matsuda Y., Sakata K., *Inorg. Chem.*, **10**, 1728—1734 (1971).
32) Yokoi H., *Bull. Chem. Soc. Jpn.*, **47**, 3037—3040 (1974).
33) Sinn E., Harris C. M., *Coord. Chem. Rev.*, **4**, 391—422 (1969).
34) Jonassen H. B., Bertrand J. A., Groves F. R. Jr., Stearns R. I., *J. Am. Chem. Soc.*, **79**, 4279—4282 (1957).
35) Yokoi H., Kishi T., *Chem. Lett.*, **1973**, 749—754.
36) James B. R., Williams J. P., *J. Chem. Soc.*, **1961**, 2007—2019.
37) Schwarzenbach G., *Helv. Chim. Acta*, **35**, 2344—2359 (1952).
38) Spike C. G., Parry R. W., *J. Am. Chem. Soc.*, **75**, 3770—3772 (1953).
39) Ishizu K., Murata S., Miyoshi K., Sugiura Y., Takita T., Umezawa H., *J. Antibiot.*, **34**, 994—1000 (1981).
40) Miyoshi K., Tanaka H., Kimura E., Tsuboyama S., Murata S., Shimizu H., Ishizu K., *Inorg. Chim. Acta*, **78**, 23—30 (1983).
41) Malmström B. G., Reinhammar B., Vänngård T., *Biochim. Biophys. Acta*, **205**, 48—57 (1970).
42) Lieberman R. A., Sands R. H., Fee J. A., *J. Biol. Chem.*, **257**, 336—344 (1982).
43) Lappin A. G., *Metal Ions in Biological Systems*, **13**, 15—71 (1981).

44) Mason H. S., *Biochem. Biophys. Res. Commun.*, **10**, 11—13 (1963).
45) Brill A. S., Bryce G. F., *J. Chem. Phys.*, **48**, 4398—4404 (1968).
46) Sutherland I. W., Wikinson J. F., *J. Gen. Microbiol.*, **30**, 105—112 (1963).
47) Broman L., Malmström B. G., Aasa R., Vänngård T., *Biochim. Biophys. Acta*, **75**, 365—376 (1963).
48) Brill A. S., Bryce G. F., Maria H. J., *Biochim. Biophys. Acta*, **154**, 342—351 (1968).
49) Suzuki H., Iwasaki H., *J. Biochem.*, **52**, 193—199 (1962).
50) Peisach J., Levine W. G., Blumberg W. E., *J. Biol. Chem.*, **242**, 2847—2858 (1967).
51) Reinhammar B. R. M., *Biochim. Biophys. Acta*, **275**, 245—259 (1972).
52) Stigbrand T., Malmström B. G., Vänngård T., *FEBS Lett.*, **12**, 260—262 (1971).
53) Stigbrand T., *FEBS Lett.*, **23**, 41—43 (1972).